

Density-functional-based predictions of Raman and IR spectra for small Si clusters

Koblar Jackson

Department of Physics, Central Michigan University, Mt. Pleasant, Michigan 48859

Mark R. Pederson

Naval Research Laboratory, Washington, D.C. 20375-5345

Dirk Porezag, Zoltan Hajnal, and Thomas Frauenheim

Institut für Physik, Technische Universität Chemnitz, D09009 Chemnitz, Germany

(Received 8 August 1996)

We have used a density-functional-based approach to study the response of silicon clusters to applied electric fields. For the dynamical response, we have calculated the Raman activities and infrared (IR) intensities for all of the vibrational modes of several clusters (Si_N with $N=3-8, 10, 13, 20,$ and 21) using the local density approximation (LDA). For the smaller clusters ($N=3-8$) our results are in good agreement with previous quantum-chemical calculations and experimental measurements, establishing that LDA-based IR and Raman data can be used in conjunction with measured spectra to determine the structure of clusters observed in experiment. To illustrate the potential of the method for larger clusters, we present calculated IR and Raman data for two low-energy isomers of Si_{10} and for the lowest-energy structure of Si_{13} found to date. For the static response, we compare our calculated polarizabilities for $N=10, 13, 20,$ and 21 to recent experimental measurements. The calculated results are in rough agreement with experiment, but show less variation with cluster size than the measurements. Taken together, our results show that LDA calculations can offer a powerful means for establishing the structures of experimentally fabricated clusters and nanoscale systems.

[S0163-1829(97)01303-9]

I. INTRODUCTION

A key challenge in the study of atomic clusters is to determine the arrangement of the atoms in the clusters. Since direct experimental observations of cluster structures are typically not possible, a combination of theoretical calculations and indirect experimental measurements must be used to definitively establish the structures. One approach involves vibrational spectroscopy. Here the frequencies observed in an IR or Raman experiment are matched against frequencies calculated for a candidate structure. Recent work using Raman¹ and IR (Ref. 2) spectroscopy combined with *ab initio* quantum-chemistry (QC) calculations was successful in determining the structures of $\text{Si}_3 - \text{Si}_7$. A crucial ingredient in this work was the theoretical prediction of the IR intensity and Raman activity of the various vibrational modes. Unfortunately, QC techniques become prohibitively complex for clusters much larger than Si_7 . However an alternative method (Ref. 3), based on the density-functional theory (DFT),^{4,5} has recently been shown to yield accurate results for hydrocarbon molecules.³ Further, because of the computational efficiency of approximations based on DFT this methodology has been successfully applied to significantly larger clusters with as many as 20–40 atoms.^{6,7}

In this paper we use this technique to calculate the IR and Raman response of small Si clusters, as well as their static polarizabilities. For the smaller clusters, we find that the DFT-based results are in good agreement with the previous QC calculations and with experiment, establishing that DFT-based IR and Raman data can be combined with experimental measurements to identify cluster structures. To illustrate

the potential of this method, we compute the IR and Raman spectra for two low-energy isomers of Si_{10} and for the most stable Si_{13} structure that has been proposed in the literature.

A large body of results has demonstrated the accuracy of the local-density approximation (LDA) in predicting structural properties such as bond lengths and bond angles.⁸ In addition, LDA-based vibrational frequencies rival those computed with QC techniques in terms of their agreement with experiment. The LDA calculations described below were carried out using an all-electron Gaussian orbital formulation. The codes feature a numerical integration scheme⁹ which ensures high accuracy in the cluster total energies and forces.¹⁰ The Perdew-Zunger form of the exchange-correlation functional was used in all the LDA calculations.¹¹ For completeness, we have also used the generalized gradient approximation (GGA) of Perdew and Wang.¹² As discussed in more detail below, we find the GGA results to be very similar to those obtained with the LDA.

Cluster geometries were optimized using a conjugate gradient algorithm, with starting point geometries taken from the literature.^{13,14} The vibrational modes for the optimized clusters were computed in the harmonic approximation by constructing and diagonalizing the Hessian matrix.¹⁵ The matrix elements were obtained from finite differences of the atomic forces computed by systematically displacing the atoms of the cluster, making full use of the cluster symmetry to reduce the computational demands.³

The IR intensity and Raman activity of the vibrational modes are determined, respectively, by how the electric dipole moment and polarizability tensor of the system change with the atomic oscillations. To the lowest order, the re-

quired quantities are proportional to the derivatives of the dipole moment and polarizability with respect to the vibrational normal modes of the cluster, evaluated at the equilibrium geometry. The IR intensity of the i th vibrational mode is given by¹⁶

$$I_i^{\text{IR}} = \frac{N\pi}{3c} \left[\frac{d\mu}{dQ_i} \right]^2.$$

Here N is the number of clusters per unit volume, μ is the cluster dipole moment, and Q_i is the normal coordinate corresponding to the i th mode. The units of I_i^{IR} are $(\text{D}/\text{\AA})^2/\text{amu}$.

The differential cross section for Raman scattering in the i th mode is¹⁷

$$\left(\frac{d\sigma}{d\Omega} \right)_i = \frac{\omega^4}{c^4} \frac{h}{4\pi\omega_i} \frac{I_{\text{Ram}}}{45}, \quad I_{\text{Ram}} = 45(\alpha')^2 + 7(\beta')^2,$$

$$\alpha' = \frac{1}{3} \left(\frac{d\alpha_{xx}}{dQ_i} + \frac{d\alpha_{yy}}{dQ_i} + \frac{d\alpha_{zz}}{dQ_i} \right),$$

$$\beta' = \frac{1}{2} \left[\left(\frac{d\alpha_{xx}}{dQ_i} - \frac{d\alpha_{yy}}{dQ_i} \right)^2 + \left(\frac{d\alpha_{xx}}{dQ_i} - \frac{d\alpha_{zz}}{dQ_i} \right)^2 + \left(\frac{d\alpha_{yy}}{dQ_i} - \frac{d\alpha_{zz}}{dQ_i} \right)^2 \right] + 3 \left[\left(\frac{d\alpha_{xy}}{dQ_i} \right)^2 + \left(\frac{d\alpha_{xz}}{dQ_i} \right)^2 + \left(\frac{d\alpha_{yz}}{dQ_i} \right)^2 \right].$$

Here ω is the frequency of the scattered radiation, ω_i is the frequency of the i th vibrational mode, and α is the polarizability tensor. The above equation assumes the standard experimental arrangement in which the scattered light is observed at a direction that is perpendicular to both the direction and polarization of the incident beam. I^{Ram} is the Raman scattering activity, typically given in units of $\text{\AA}^4/\text{amu}$. The above expression for I^{Ram} is appropriately averaged over all cluster orientations. The depolarization ratio for the scattered light is given by

$$\rho = \frac{3\beta'^2}{45\alpha'^2 + 4\beta'^2}.$$

To obtain the IR and Raman data, we must compute the dipole and polarizability derivatives with respect to the normal mode coordinates. These can be viewed as directional derivatives in the space of $3N$ nuclear coordinates and expressed, using the chain rule, in terms of derivatives with respect to atomic coordinates (R_k). For an arbitrary function A ,

$$\frac{dA}{dQ_i} = \sum_{k=1}^{3N} \frac{\partial A}{\partial R_k} X_{ki},$$

where X_{ki} is the k th atomic displacement of the i th normal mode. The necessary derivatives can be expressed in terms of the atomic forces as follows:

$$\frac{\partial \mu_i}{\partial R_k} = - \frac{\partial^2 E}{\partial G_i \partial R_k} = \frac{\partial F_k}{\partial G_i},$$

$$\frac{\partial \alpha_{ij}}{\partial R_k} = - \frac{\partial^3 E}{\partial G_i \partial G_j \partial R_k} = \frac{\partial^2 F_k}{\partial G_i \partial G_j},$$

where E is the cluster total energy, G_i is the i th component of an assumed external electric field, and F_k is the calculated force on the k th atomic coordinate. We obtain the derivatives by taking finite differences of the forces from independent self-consistent calculations with an applied electric field. This approach was introduced by Komornicki and McIver.¹⁸

Benchmark calculations on a series of hydrocarbon molecules plus water³ indicate that absolute IR intensities and Raman activities with typical deviations of 30–50 % from experiment can be obtained with this LDA-based approach. Roughly similar results for the Raman activities were found in a different preliminary study using the same basic approach.¹⁹

We have found that the key numerical issues involved in accurately computing the IR intensities and Raman activities are highly self-consistent wave functions and large basis sets including adequate polarization functions.³ In addition, we have found high numerical precision, which we obtain using our numerical integration scheme,⁹ to be important in accurately finding the positions of the vibrational frequencies. To ensure good convergence in the self-consistency cycle, we converge the cluster *kinetic energy* instead of the variational total energy, using a tolerance of 0.0001 Hartree. The basis set used in the calculations reported below includes 9 s -type, 8 p -type, and 6 d -type orbitals (9,8,6) on each Si atom, contracted from a set of 15 primitive Gaussians per atom. Previously reported tests⁶ on the Si_4 cluster indicate that the vibrational frequencies, the IR intensities, and the Raman activities are well-converged using this basis.

II. SMALL SILICON CLUSTERS: Si_3 - Si_8

A. The infrared intensities

For Si_3 through Si_8 , we studied the lowest-energy structures found by Fournier *et al.*,¹³ in their extensive LDA study of small Si clusters. We used the bond lengths quoted in Ref. 13 to generate starting point geometries, and then relaxed the clusters to their minimum-energy geometries using our codes. In all cases the relaxation was small, with bond lengths changing typically by a percent or less. The small differences can be attributed to the use of different exchange-correlation functionals. Fournier *et al.*¹³ used the functional of Vosko, Wilkes, and Nusair.²⁰ Our computed vibrational frequencies are also in very good agreement with Fournier *et al.* For convenience, we show the relaxed cluster structures in Fig. 1.

In Table I we give the frequencies and IR intensities of the IR active modes computed for the small Si clusters. For Si_3 - Si_7 we also give the QC results and the experimentally observed frequencies quoted in the paper of Li *et al.*² In that work, the geometry and vibrational frequencies were computed at a high level of theory, including electron correlation directly for the smaller clusters and perturbatively for the larger clusters. The IR intensities were computed at the Hartree-Fock (HF) level, using more extensive basis sets.

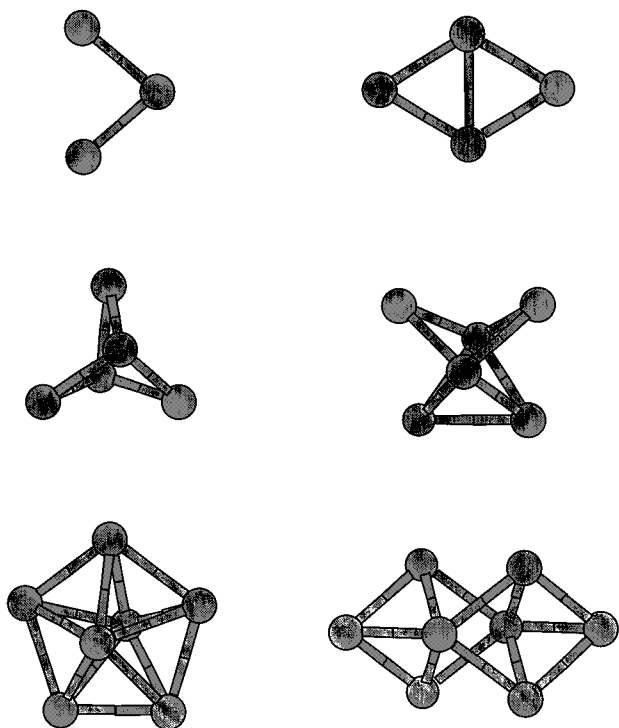


FIG. 1. Pictured above are the lowest-energy geometries that we have found for Si_3 - Si_8 and the geometries for which we have calculated the infrared and Raman spectra.

The results in Table I show very good agreement between the frequencies computed using the two techniques, with typical differences of approximately 10 cm^{-1} . For the absolute IR intensities, quoted in units of $(\text{D}/\text{\AA})^2/\text{amu}$, the LDA results are systematically smaller than the quantum-chemistry results by a factor of 2–3. [The latter were quoted in Ref. 2 in km/mol and converted using the standard conversion $1 (\text{D}/\text{\AA})^2/\text{amu} = 42.255 \text{ km/mol}$.] The differences may be due to the fact that the QC intensities were calculated at the HF level. Extensive studies on small molecules²¹ have shown that HF tends to significantly overestimate IR intensities.

Despite the quantitative differences, the LDA and QC IR intensities are in very good qualitative agreement. In particular, the calculations agree completely on which are the most active modes for each cluster. It is interesting to note that only the modes corresponding to intensities greater than or equal to $0.20 (\text{D}/\text{\AA})^2/\text{amu}$ (in the LDA results) could be identified in the experimental spectra of Ref. 2. The average of the QC:LDA intensity ratio for these observed modes is 2.4. If we multiply the LDA intensities by this common factor to consider the agreement of the relative intensities, we find that the average difference between the LDA and QC is only about 10% for the strong modes.

The IR results for Si_5 stand out as a clear exception to the agreement described above. For this cluster, the QC calculations predict two strong IR modes at 436 and 382 cm^{-1} . The LDA calculations predict IR active modes close to these frequencies, at 444 and 412 cm^{-1} , but the LDA predicts these modes to be *very weak*. Electron correlation effects may be responsible for the qualitative differences seen in this case. Li *et al.*, note that the calculated QC bond lengths and vibra-

TABLE I. Comparison of absolute IR intensities calculated within the LDA (this work) and by quantum-chemistry techniques (Ref. 2), along with the observed IR-active frequencies (Ref. 2). Frequencies (ω) are in units of cm^{-1} and IR intensities are in units of $(\text{D}/\text{\AA})^2/\text{amu}$.

	LDA		HF		Expt. ω
	ω	IR	ω	IR	
Si_3	173	0.09	148	0.21	
	536	0.80	525	1.41	525
	546	0.20	551	0.47	550.6
Si_4	53	0.12	101	0.05	
	249	0.03	239	0.19	
	496	1.34	499	3.85	501
Si_5	174	0.05	160	0.05	
	412	0.07	382	0.51	
	444	0.04	436	1.81	
Si_6	51	0.01	049	0.02	
	319	0.01	340	0.10	
	410	0.01			
	463	0.84	458	2.07	461
Si_7	240	0.01	249	0.07	
	430	0.54	421	1.41	422
Si_8	147	0.01			
	168	0.01			
	302	0.06			
	365	0.03			
	398	0.15			
	518	0.15			

tional frequencies for Si_5 depend sensitively to the treatment of electron correlation, suggesting that a correlation-related effects are particularly strong for this system. The use of HF wave functions to compute the IR intensities may thus be a poor approximation in this case.

Interestingly, no modes found in the experimental spectra of Ref. 2 could be assigned to Si_5 , despite the predicted strength of the active modes. Li *et al.* attributed this to a low concentration of Si_5 clusters in the experiment. Our results suggest another possible explanation: the Si_5 clusters were present in reasonable numbers in the experiment, but with IR modes too weak to detect.

It is interesting to compare the IR results obtained using the LDA and a recently proposed generalized gradient approximation (GGA) to DFT.¹² Generally speaking, GGA's were introduced to correct the tendency of the LDA to overbind molecules with respect to isolated atoms. Most studies confirm that this is the main effect, with other properties such as bond lengths and electronic densities remaining relatively unchanged. For example, use of the GGA gives rise to little change in the bond lengths or the vibrational frequencies of benchmark molecules studied in Ref. 3; however, a slight improvement in comparison to experiment was found for the IR intensities. For Si_3 - Si_8 we find that the GGA bond lengths are slightly longer by about 1% compared to the LDA, and typical vibrational frequencies are softer by about 10 cm^{-1} . The GGA IR intensities and Raman activities are very similar to the LDA counterparts, with typical differences less than 10%. In this case the GGA appears to

TABLE II. Comparison of relative Raman activities calculated within the LDA (this work) and by quantum-chemistry techniques (Ref. 1), along with the observed Raman-active frequencies (Ref. 1). The relative units are computed separately for each cluster; absolute activities cannot be inferred when comparing modes from different clusters. Frequencies are in cm^{-1} and activities are in relative units.

	LDA		MP2		Expt.
	ω	I_{RAM}	ω	I_{RAM}	ω
Si ₃	173	1.00			
	536	0.27			
	546	2.61			
Si ₄	346	1.00	337	1.00	345
	436	0.40	440	0.5	
	470	3.9	463	5.0	470
Si ₅	174	1.0			
	234	0.9			
	382	0.7			
	443	0.7			
	476	6.7			
Si ₆	270	1.0	209	1.0	252
	315	1.3	298	2.6	300
	384	1.0	376	0.6	386
	412	0.8	425	2.0	404
	463	7.9	457	7.7	458
Si ₇	301	1.0	300	1.0	289
	347	1.8	339	0.5	340
	347	1.4	346	0.5	340
	362	4.5	352	1.6	358
	448	9.2	441	4.1	435
Si ₈	105	0.4			
	225	1.0			
	257	0.6			
	292	1.0			
	314	0.3			
	318	3.2			
	348	0.6			
	404	5.1			
515	2.2				

give no systematic improvement over the LDA in comparison to either experiment or the QC calculations. We therefore show only the LDA results in Table I.

B. The Raman activities

In Table II we present our calculated Raman activities, comparing them with the QC results given in Ref. 1. The Raman activities are given in relative units, following Ref. 1, and only the Raman-active modes are shown. We also give the positions of the Raman-active modes found in the experiment.¹

The LDA and QC are in excellent agreement regarding the positions of the Raman-active modes; typical differences are about 10 cm^{-1} . The relative activities show quantitative differences as large as roughly 100% for the strongest modes, but are in complete agreement in identifying the strong Raman modes. Note that only the strong modes were

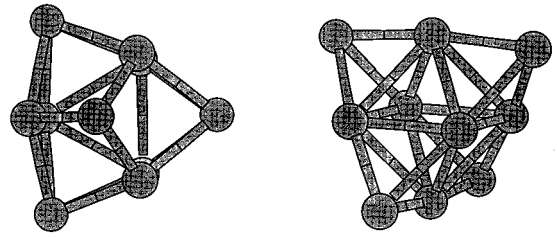


FIG. 2. Pictured above are two candidates for the lowest Si₁₀ structures. We find that the TTP structure (left) lies lower than the TCO structure by 0.67 eV.

observed in the experiments. It can thus be seen that the LDA results could have been used to identify the cluster structures in the experiments.

III. THE RAMAN AND INFRARED SIGNATURES OF Si₁₀ ISOMERS

We have applied our formalism to Si₁₀. The ground state structure of this cluster has not been completely established. Ballone *et al.*²² and Rohlffing and Raghavachari¹⁴ suggested a tetracapped trigonal prism (TTP) as the lowest-energy structure, lying below a tetracapped octahedron (TCO) proposed by Tomanek and Schlüter.²³ In the QC calculation, however, the relative ordering of the two structures depended on the treatment of electron correlation,¹⁴ thus raising a question as to the true ordering of the structures. We find the TTP structure to lie 0.67 eV below the TCO. This is in good agreement with the energy difference of 1.04 eV found by Raghavachari and Rohlffing¹⁴ at the MP4 level of theory and in excellent agreement with the 0.67 eV difference found by Ordejon *et al.*,²⁴ in a recent nonorthogonal tight-binding calculation. The relaxed structures for the TTP and TCO clusters are shown in Fig. 2.

In Fig. 3, we present predicted IR and Raman spectra for the TTP and TCO structures. In the lower panel is a Gaussian-broadened vibrational density of states (VDOS) plot, obtained by centering a Gaussian with a full width at half maximum of 6 cm^{-1} on each of the normal mode frequencies and multiplying by the degeneracy of the mode. In the second and upper panels, respectively, the VDOS is weighted by the IR intensity and Raman activities of the various modes. For the Raman spectra we show the activity for parallel and perpendicular polarizations. The predicted Raman spectra for the two structures are very similar. The TCO and TTP structures both exhibit a prominent, polarized Raman-active peak at 367 cm^{-1} and 381 cm^{-1} , respectively. Since 20 cm^{-1} deviations between LDA and experiment are not uncommon these polarized peaks are probably not useful for identifying the Si₁₀ geometry in experiments. Both structures exhibit two unpolarized Raman peaks at lower energies. The unpolarized peak at 294 cm^{-1} for the TCO cluster may be observable experimentally.

In contrast to the Raman spectra, the calculated IR spectra shown in the second panel of Fig. 3 are strikingly different. The TCO spectrum has a single, very strong mode at 531 cm^{-1} . The absolute IR intensity of this mode is about $1.5 (\text{D}/\text{\AA})^2/\text{amu}$, making it stronger than any of the modes computed for Si₃ - Si₈. (See Table I.) By contrast, the prominent

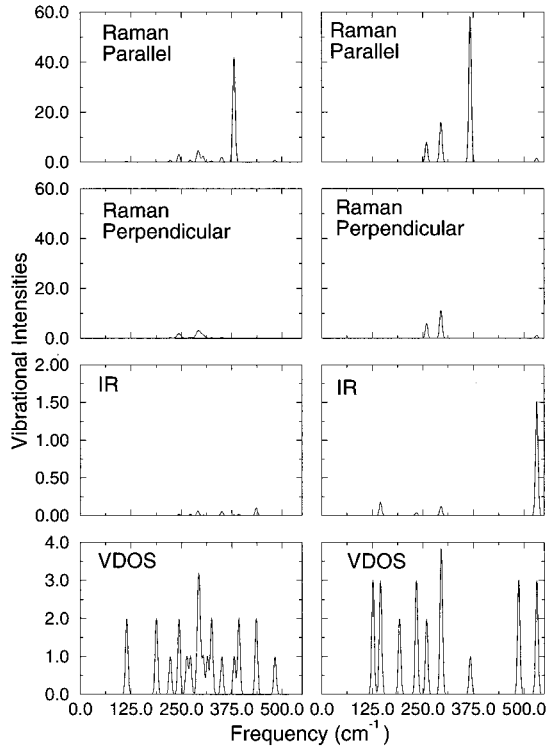


FIG. 3. Comparison of the vibrational density of states (VDOS) and simulated IR and Raman spectra for the two Si_{10} structures shown in Fig. 2. The TTP and TCO structures correspond to the left and right panels, respectively. The VDOS was obtained using a 6 cm^{-1} Gaussian broadening and the computed normal mode frequencies. The simulated IR and Raman spectra (for parallel and perpendicular polarizations) were obtained by weighting the VDOS data with the IR intensity and Raman activity, respectively, of the various modes.

IR modes for the TTP structure lie at 436 , 291 , and 351 cm^{-1} ; however, these modes are predicted to be more than an order of magnitude weaker than the TCO mode, and thus potentially difficult to observe in experiment.

Considering that we find the TTP structure to be 0.67 eV more stable than the TCO structure, we can summarize our prediction of the vibrational signature of Si_{10} : It should consist of a single strong polarized Raman line at around 381 cm^{-1} , a broad but weak unpolarized Raman peak between 272 and 304 cm^{-1} , a sharper and weaker unpolarized Raman peak at 244 cm^{-1} , and a very weak IR spectra. The broad Raman peak from 272 – 304 cm^{-1} is due to six different vibrational modes and depending on the experimental resolution could appear as a two-peaked structure.

IV. THE RAMAN AND IR SIGNATURES OF Si_{13} CLUSTERS

We have relaxed several Si_{13} isomers, concluding that the most stable structure is the one found by R othlisberger²⁵ (see Fig. 4) using simulated annealing techniques. This result is in good agreement with recent quantum Monte Carlo calculations.²⁶ The most striking property of the cluster is its unusually large electronic gap (calculated at 1.60 eV within LDA). Figure 4 shows the corresponding IR spectrum, Raman spectra, and vibrational density of states as calculated

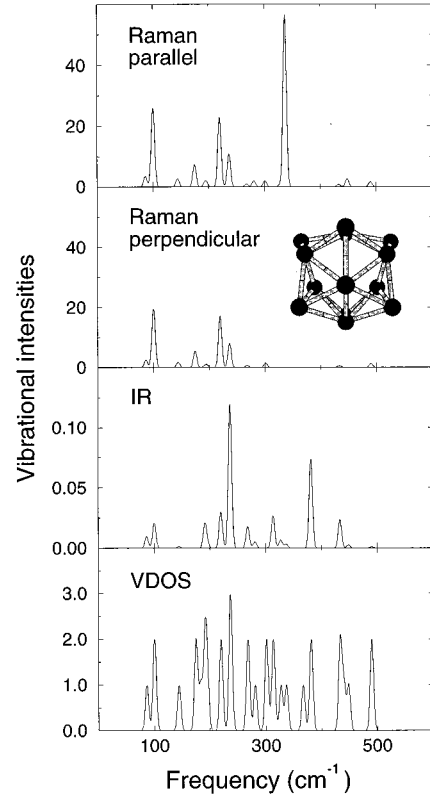


FIG. 4. The vibrational density of states (VDOS), IR and Raman spectra for the Si_{13} cluster. Both the parallel and perpendicular Raman spectra are shown.

within LDA. We show both the parallel and perpendicular Raman spectra. The IR response is rather weak [the strongest mode at 236 cm^{-1} has an absolute intensity of only $0.12 (\text{D}/\text{Å})^2/\text{amu}$]. The strongest Raman mode (calculated at 337 cm^{-1}) is fully polarized as can be seen by comparing the parallel and perpendicular polarization spectra. Other strong modes appear at 100 cm^{-1} , 174 cm^{-1} , 220 cm^{-1} , and 236 cm^{-1} .

V. POLARIZABILITIES OF SILICON CLUSTERS

In a recent paper, Sch afer *et al.* have measured the polarizabilities of silicon clusters for sizes ranging between $N=9$ and $N=50$ atoms.²⁸ A striking result described in this paper was a strong variation of the polarizability per atom as a function of cluster size. To address this point theoretically we have computed the static polarizabilities for the silicon atom as well as our Si_{10} , Si_{13} , Si_{20} , and Si_{21} clusters within the LDA.³⁰ A comparison between our results and the experimental results is presented in Table III. For the single atom, the deviation between theory and experiment is 0.5 \AA^3 or 10% which, as discussed below, is what is expected from previous applications of density-functional theory to such problems. However for the clusters, the average deviation between the theoretical results and the experimental results is 1.36 \AA^3 which is slightly larger than the typical experimental uncertainty of 0.8 \AA^3 quoted in Ref. 28. While there is some agreement on the deviations as a function of cluster size, the theoretical results tend to favor smaller variations with size than were observed experimentally. The

TABLE III. Comparison of calculated and measured polarizabilities for Si₁₀, Si₁₃, Si₂₀, and Si₂₁. Experimental results are from Ref. 27 for the atom and Ref. 28 for the clusters. Units are in Å³ per atom for polarizabilities and debye for dipole moments.

Cluster	$ \mu_{\text{LDA}} $	α_{LDA}	$\alpha_{\text{Expt.}}$
Si ₁	0.00	5.88	5.38
Si ₁₀	0.72	4.34	5.50
Si ₁₃	0.12	4.40	1.75
Si ₂₀	0.02	4.83	3.63
Si ₂₁	0.79	4.58	3.10

large deviations between theory and experiment seen in Table III stand in contrast to the 5–10 % agreement between LDA calculations and experimental polarizations for noble gas atoms,²⁹ hydrocarbon and H₂O molecules,³ and fullerene and benzene molecules.³⁰ Some of the differences in Table III may be due to our choice of cluster models. The structures for these clusters have not been definitively determined, so that our calculated polarizabilities may be for structures different than the ones observed in the experiments. This is particularly true for the larger clusters ($N=20$ and 21); however, the structures used for $N=10$ and 13 have resulted from extensive theoretical searches for the optimal structures and are thus good candidates for the ideal structures. It will be particularly interesting to conclusively determine the structure of these clusters, perhaps with the help of the Raman and IR spectra predicted here, in order to better understand the differences in the theoretical and experimental polarizabilities.

VI. SUMMARY

We have used the LDA to calculate the *experimentally observable* static and dynamical responses of silicon clusters in the presence of external electric fields. For the $N=3-8$ size range we have made a detailed comparison with previous quantum-chemical-based calculations and with

existing experimental data, finding good agreement with the previous work. These results show that theoretically determined vibrational spectra based on density functional theory can be used in conjunction with experimental measurements to characterize cluster structures. In contrast to earlier work on hydrocarbons,³ we did not observe significant improvements of the GGA over the LDA for infrared spectra. An advantage of the density-functional-based approach is that it can extend such calculations to cluster sizes beyond the reach of traditional QC techniques. Such a capability is especially important to the design and fabrication of new cluster assembled materials since the intermediate building blocks may be metastable rather than ground-state structures.

To illustrate the potential of the method, we applied the formalism to two candidate structures for Si₁₀, obtaining the predicted spectra given in Fig. 3, and the lowest known isomer of Si₁₃, with results given in Fig. 4. We have also recently computed predicted IR and Raman spectra for candidate structures for Si₂₀ and Si₂₁.⁶

In addition to the dynamical response we have determined the static polarizabilities of four larger clusters ($N=10, 13, 20,$ and 21). The results in Table III show significant differences between the calculated and measured polarizabilities.²⁸ Additional work, including a determination of the structure of the observed clusters, is required to fully understand these differences.

It is our hope that LDA-based calculations of Raman activities and IR intensities will be coupled with appropriate experimental measurements to make structure determinations possible for clusters well into the intermediate size range. This would be tremendously useful for studying the size evolution of cluster structure.

ACKNOWLEDGMENTS

This work was supported in part by NSF Grants Nos. RUI-DMR940985 and NSF/DAAD INT-9514714, by ONR Grant No. N00014-96-1-1116, and by the German Research Foundation.

- ¹E. Honea, A. Ogura, C. A. Murray, Krishnan Raghavachari, W. O. Sprenger, M. F. Jarrold, and W. L. Brown, *Nature (London)* **366**, 42 (1993).
- ²S. Li, R. Z. Van Zee, W. Weltner Jr., and Krishnan Raghavachari, *Chem. Phys. Lett.*, **243**, 275 (1995).
- ³D. V. Porezag and M. R. Pederson, *Phys. Rev. B* **54**, 7830 (1996).
- ⁴P. Hohenberg and W. Kohn, *Phys. Rev.* **136**, B864 (1964).
- ⁵W. Kohn and L. J. Sham, *Phys. Rev.* **140**, A1133 (1965).
- ⁶M. R. Pederson, K. A. Jackson, D. V. Porezag, Z. Hajnal, and Th. Frauenheim, *Phys. Rev. B* **54**, 2863 (1996).
- ⁷M. R. Pederson and N. Laouini, *Phys. Rev. B* **54**, 7830 (1996).
- ⁸R. O. Jones and O. Gunnarson, *Rev. Mod. Phys.* **61**, 689 (1989).
- ⁹M. R. Pederson and K. A. Jackson, *Phys. Rev. B* **41**, 7453 (1990).
- ¹⁰K. A. Jackson and M. R. Pederson, *Phys. Rev. B* **42**, 3276 (1990).
- ¹¹J. P. Perdew and A. Zunger, *Phys. Rev. B* **23**, 5048 (1979).
- ¹²J. P. Perdew, J. A. Chevary, S. H. Vosko, K. A. Jackson, M. R. Pederson, D. J. Singh, and C. Fiolhais, *Phys. Rev. B* **46**, 6671 (1992), and references therein.
- ¹³R. Fournier, S. B. Sinnott, and A. E. DePristo, *J. Chem. Phys.* **97**, 4149 (1992).
- ¹⁴C. M. Rohlfing and K. Raghavachari, *J. Chem. Phys.* **96**, 2114 (1992).
- ¹⁵A. A. Quong, M. R. Pederson, and J. L. Feldman, *Solid State Commun.* **87**, 535 (1993).
- ¹⁶E. B. Wilson, J. C. Decius, and P. C. Cross, *Molecular Vibrations* (McGraw-Hill, New York, 1955).
- ¹⁷M. Cardona, in *Light Scattering in Solids II*, Topics in Applied Physics Vol. 50 (Springer, Berlin, 1982).
- ¹⁸A. Komornicki and J. W. McIver, *J. Chem. Phys.* **70**, 2014 (1979).
- ¹⁹B. G. Johnson and J. Florian, *Chem. Phys. Lett.* **247**, 120 (1995).
- ²⁰S. H. Vosko, L. Wilk, and M. Nusair, *Can. J. Phys.* **58**, 1200 (1980).
- ²¹J. R. Thomas, B. J. DeLeeuw, G. Vacek, T. D. Crawford, Y. Yamaguchi, and H. F. Schaefer, *J. Chem. Phys.* **99**, 403 (1993).

- ²²P. Ballone *et al.*, Phys. Rev. Lett. **60**, 271 (1988).
- ²³D. Tomanek and M. Schlüter, Phys. Rev. Lett. **56**, 1055 (1986).
- ²⁴P. Ordejon, D. Lebedenko, and M. Menon, Phys. Rev. B **50**, 5645 (1994).
- ²⁵U. Röthlisberger, W. Andreoni, and P. Giannozzi, J. Chem. Phys. **92**, 1248 (1992).
- ²⁶J. C. Grossman and L. Mitas, Phys. Rev. Lett. **74**, 1323 (1995).
- ²⁷*Handbook of Chemistry and Physics*, 74th ed., edited by D. Lide (CRC Press, Boca Raton, 1993).
- ²⁸R. Schäfer, S. Schlecht, J. Woenckhaus, and J. A. Becker, Phys. Rev. Lett. **76**, 471 (1996).
- ²⁹A. Zangwill and P. Soven, Phys. Rev. A **21**, 1561 (1980).
- ³⁰M. R. Pederson and A. A. Quong, Phys. Rev. B **46**, 13 584 (1992); A. A. Quong and M. R. Pederson, *ibid.* **46** 12 906 (1992).